Oxygen isotope disequilibrium in the juvenile portion of oyster shells biases seawater temperature reconstructions

Damien Huyghe, Laurent Emmanuel, Marc de Rafélis, Maurice Renard, Michel Ropert, Nathalie Labourdette, Franck Lartaud

Oxygen isotope disequilibrium in the juvenile portion of oyster shells biases seawater temperature reconstructions

Damien Huyghe[1,2,3 *], Laurent Emmanuel[4], Marc de Rafelis[2], Maurice Renard[4], Michel Ropert[5], Nathalie Labourdette[4], Franck Lartaud[1]

[1] Sorbonne Université, CNRS, Laboratoire d'Ecogéochimie des Environnements Benthiques, LECOB, F-66650, Banyuls-sur-mer, France

[2] Géosciences Environnement Toulouse, CNRS, IRD, Université Paul Sabatier Toulouse 3, 14 Avenue Edouard Belin, 31400 Toulouse, France

[3] Now at MINES ParisTech, PSL University, Centre de Géosciences, 35 rue St Honoré, 77305 Fontainebleau Cedex, France

[4] Sorbonne Université, CNRS-INSU, Institut des Sciences de la Terre Paris, ISTeP, F-75005 Paris, France

[5] Ifremer, Laboratoire Environnement Ressource de Normandie, Avenue du Général de Gaulle, BP 32, 14520 Port-en-Bessin, France

* corresponding author: Damien Huyghe (damien.huyghe@mines-paristech.fr)

Abstract

For decades, bivalve shells have constituted one of the most common supports for paleoclimatic archives based on stable isotope approaches. In this work, we conducted chemical marking and recapture techniques to study the fluctuation of $\delta^{18}O$ values of oyster shells of the species *Magallana gigas* reared in natural environment in Normandy (France) for two years. The results were compared to the continuous monitoring of temperature and salinity and monthly records of seawater $\delta^{18}O$. Isotopic measurements were performed on the hinge area that regroups the whole life of the oysters. Here we demonstrate that oysters mineralized their shells with no significant growth breaks during the two-years experiment, even at temperatures below 6 °C. The results confirm that adult oysters (i.e. > 1 yr) mineralized their shells at equilibrium. However, juvenile specimens exhibit a strong isotopic disequilibrium, with a maximum shift of the $\delta^{18}O$ values of 3 ‰ in winter, likely due to kinetic isotope effects. This corresponds to a reconstructed temperature up to 13 °C warmer than expected. This work indicates that although these oyster shells can be used as an accurate archive of (paleo)environmental conditions, the shell portion mineralized during the juvenile stage (i.e. < 1 yr) should be avoided for paleotemperature reconstructions. Given the wide use of bivalve shells as environmental archives, similar studies on others species are required.

Keywords: stable isotopes; paleoclimatology; sclerogeochemistry; sclerochronology; kinetic isotope effect

1. Introduction

Since the precursor works of Urey (1947) and Epstein et al. (1951), measurement of the oxygen stable isotope composition of carbonates, namely $\delta^{18}O$, has been the most common approach used to reconstruct past seawater temperatures. These works have shown that in calcium carbonate minerals, the $\delta^{18}O$ value is a function of both the temperature and the $\delta^{18}O$ composition of seawater ($\delta^{18}O_w$). In shallow marine environments, this method has been broadly applied to mollusks, as they are potentially long-living organisms and the high-resolution measurement of the $\delta^{18}O$ value of their shells ($\delta^{18}O_{shell}$) allows for the reconstruction of present and past seasonal gradients of seawater temperatures (e.g. Jones and Quitmyer, 1996; Purton and Brasier, 1997; Kirby et al., 1998; Surge et al. 2001, 2003; Kobashi et al., 2001; Latal et al., 2004; Schöne et al., 2004; Lartaud et al., 2010a; Harzhauser et al., 2011; Wanamaker et al., 2012; Mette et al., 2016; Reynolds et al., 2017; Briard et al., 2020).

One of the prerequisites for using $\delta^{18}O$ values for (paleo)environmental reconstructions is to determine if the organisms mineralize their shell in isotopic equilibrium with seawater. So-called isotopic disequilibrium has been identified for taxa, such as the coccolithophores, foraminifers or corals (McConnaughey et al., 1997; Spero et al., 1997; Adkins et al., 2003; Hermoso et al., 2016). Isotopic disequilibria are on the contrary reputed to be nonexistent or negligible for most marine mollusk species (Wefer and Berger, 1991; Chauvaud et al., 2005; Schöne et al., 2005; Peharda et al., 2019), although exceptions have been reported for some species, such as deep sea oysters of the genius *Pycnodonte* (Wisshak et al., 2009) or the giant scallop, *Pecten maximus* (Owen et al., 2002). Kinetic isotope effects induced by anomalously low or high growth rates have been proposed by these authors, in addition to the combined effects of environmentally 'stressful' conditions (e.g., low

temperature, low salinity), as causes of disruptions in isotopic equilibrium (Owen et al., 2008; Lartaud et al., 2010c). Finally, a recent study demonstrates that most of biogenic carbonates do not unequivocally precipitate at isotopic equilibrium and suggests revising the classic thermodynamic model (Daëron et al., 2019).

In depth work is thus required to characterize the conditions under which mollusks form their shells at isotopic equilibrium. Among the mollusk shells used as environmental archives, shallow-water oysters are considered as important model species, as many studies have shown that their oxygen stable isotope signature can provide reliable information about their living conditions using oxygen stable isotopes geochemistry (Wefer and Berger, 1991; Richardson et al., 1993; Kirby et al., 1998; Surge et al. 2001, 2003; Lécuyer et al., 2004; Lartaud et al., 2010a, 2010b; Ullmann et al. 2010; Tynan et al. 2014), or magnesium-calcium ratios (Surge and Lohmann, 2008; Mouchi et al., 2013; Tynan et al., 2017). Oysters are ubiquitous and abundant organisms found in shallow marine and brackish deposits since the Jurassic and mineralize their shells with calcite materials, making them resistant to diagenesis. Oyster shells are thus commonly used to reconstruct the mean annual and seasonal gradient of paleotemperatures of near shore environments (Kirby et al., 1998; Kirby, 2000, 2001; Brigaud et al., 2008; Lartaud et al., 2010a; Harzhauser et al., 2011; Huyghe et al., 2012; Briard et al., 2020).

To use shell material as a (paleo)environmental parameter archive, a precise growth chronology allowing to properly refer each carbonate micro-sampling to a calendar date must be determined. This type of approach is widely used in bivalve shells such as *Arctica islandica* or *Pecten maximus* that mineralize one increment each year and each day during part of the year respectively (Schöne et al., 2004; Chauvaud et al., 2005; Mette et al., 2016). On the contrary, it was demonstrated that oysters do not precipitate calcitic increments at regular time intervals throughout their life (i.e., several growth anomalies were reported

during the juvenile period while growth is strongly tidal related after; Huyghe et al., 2019). Thus, to get around this limit, we used mark and recapture experiments based on regular chemical staining of shells, combined with sclerochronological techniques (Lartaud et al., 2010d; Nedoncelle et al., 2013). The resulting shell growth model revealed under cathodoluminescence (CL) observations, demonstrated the validity of using this type of biogenic material (Langlet et al., 2006; Lartaud et al., 2010d). This growth model, significantly revised by Huyghe et al. (2019) provides a suitable framework to test if mineralization occurs in isotopic equilibrium during the entire specimen lifetime. .

2. Materials and methods

2.1. The Magallana gigas oyster

This work focuses on the analysis of oysters of the species *Magallana gigas*, which corresponds to the former *Crassostrea gigas* (Salvi and Mariottini, 2017). These oysters are widely raised commercially in shallow water environments. They tolerate large variations of water salinity, temperature and turbidity. *Magallana gigas* oysters are suspension feeders and sequentially hermaphrodites, reaching sexual maturity at 12 to 18 months in the studied area (Soletchnik et al., 1996). Reproduction occurs during summer on the French Atlantic coast, but in the location of this work, in the English Channel, the temperature generally remains too cold for reproduction (Ropert et al., 2007), which forces shellfish-farmers to import spats from more southern French locations. In the present study, we consider specimens of less than 12 months as juveniles (i.e. before summer 2005) and specimens older than 12 months as sub-adults according to the age when sexual maturity starts for these oysters.

121

122 *2.2. Breeding site and breeding conditions*

123

124 Young oysters (< 6 months old) were reared for 2 years in an experimental site of the
125 *Institut Français de Recherche pour l'Exploitation de la Mer* (IFREMER), located on the
126 Normandy coast of the English Channel, at the Baie des Veys (BDV, 49°23.110'N
127 1°6.050'W), following the protocol described in Lartaud et al. (2010d). The BDV is an open
128 bay characterized by a high intertidal setting and semi-diurnal tide regime (Huyghe et al.,
129 2019). Young (< 6 months) and small-sized (< 2 cm) specimens of *M. gigas* were collected
130 from wild broodstock at the Arcachon Basin (Gironde, France), at the end of January 2005
131 and were then transferred to the BDV for growth experiments. The shells were cultivated on
132 oyster tables from the January 28, 2005 to November 28, 2006. Oysters were reared on tables
133 50 cm above the sediment. Maximum water depth was 6m above the tables and they were
134 emerged during maximum 3 hours per day during periods of low waters spring tides (Huyghe
135 et al., 2019). Hourly measurements of seawater temperature and salinity were directly
136 conducted at the sampled oyster for this study using a multi-parameter probe (YSI data
137 logger, IFREMER) from January 2005 to November 2006 (Huyghe et al., 2019; Fig. 1). The
138 water temperature on the oyster tables ranged from 4.8 to 20 °C and fluctuated seasonally
139 with mean summer (July to September) and winter (January to March) temperatures of
140 18.7±0.6 and 6.7±1.1 °C respectively (Huyghe et al., 2019; Fig. 1). Salinity remained quite
141 stable over the year (33.3±0.7) and displayed only episodic freshwater inputs, which reduced
142 values to 28.8, following heavy rainfalls (Fig. 1).

143 To assign a growth calendar and link the isotope records of biogenic calcite material
144 with the fluctuation of the environmental parameters, we used a mark and recapture technique
145 combined with the sclerochronological analysis of shells (Lartaud et al., 2010d; Huyghe et al.,

2019). Oyster shells were stained at nearly regular intervals (i.e., 15 times during the whole breeding phase) on site with Mn^{2+} following the protocol of Langlet et al. (2006). For each staining, oysters were immersed for 4 hours during low tide in a tank filled with seawater in which 90 $mg.l^{-1}$ of manganese chloride tetrahydrate ($MnCl_2$. $4H_2O$) was added. Oysters were sampled in November 2006 and shells were then sectioned and mounted on thin sections for CL observations. Rapid incorporation of Mn^{2+} into the shell calcite appeared as highly luminescent micro-growth bands under CL (Fig. 2; Langlet et al., 2006; Barbin et al., 2008). The identification of the successive Mn^{2+}-markings and the use of tidal CL increments in shell sections allowed for the determination of growth rates over the corresponding time intervals and the identification of a high-resolution calendar growth profile (Fig. 2; Huyghe et al., 2019).

2.3. Shell preparation and isotope analyses

Immediately upon collection, the oysters were carefully opened and the flesh was scrapped and removed from the inner surface of the shell valves. Upon return to the laboratory, the shells were placed in a 6 % solution of hydrogen peroxide (H_2O_2) for 6 hours to remove any epibionta from the outer shell surfaces, washed in 0.15 N nitric acid for 20 minutes to dissolve any carbonate based superficial contamination and rinsed in demineralized water. Observations and samplings were made on the hinge area of the oysters that compiles a complete ontogenetic record of both oyster hinge growth and environmental conditions experienced throughout their lives (Lartaud et al., 2010d). The dry left valve of the shell was cut longitudinally along the growth axis at the umbo region, and thin sections were manufactured to expose the preserved internal structures in order to perform CL observation of the foliated low-magnesium calcite of the hinge region. Mn^{2+} markings were revealed

171 under CL microscopy observations (Fig. 2) with a cold cathode (Cathodyne-OPEA, 15-20 kV
172 and 200-300 µAm.mm^{-2} under a pressure of 0.05 Torr).

173 Shell calcium carbonate samples for $\delta^{18}O_{shell}$ analyses were drilled to a depth of 100
174 µm along each thin section growth profile in the hinge region. We used a 0.3 mm drill bit and
175 a computer assisted micromill. Samplings were performed at low and constant speed. The
176 corresponding dates for each drilled sample were assigned using the CL growth profile
177 previously described (Fig. 2). The collected carbonate powders were acidified in 100 %
178 H_3PO_4 at 50 °C under vacuum. The CO_2 produced was collected and analyzed using a VG
179 Instruments Isoprime mass spectrometer. Isotopic data were reported in conventional delta (δ)
180 notation relative to the Vienna Pee Dee Belemnite (VPDB). The standard used for the
181 analyses was an internal standard calibrated on the NBS-19. Standard deviation for $\delta^{18}O$
182 values was ± 0.1 ‰.
183
184 *2.4. $\delta^{18}O$ seawater analyses*
185
186 Sub-monthly analyses of seawater oxygen isotopic composition ($\delta^{18}O_w$) were also
187 performed to determine their seasonal variation. We used the method described in Pierre et al.
188 (1994) for water sampling and analyses. The water samples were collected during high tides,
189 above the oyster tables, in 100 ml glass bottles. CO_2-water equilibration method of Epstein
190 and Mayeda (1953) was used as the analytical procedure for the CO_2 preparation in order to
191 measure the $\delta^{18}O_w$ values.

192 The isotopic compositions were determined using a VG Micromass 602 mass
193 spectrometer. The analytical reproducibility was within the range 1σ = 0.1‰ for $\delta^{18}O$ values.
194 The δ values correspond to the per mil deviation of the sample relative to the SMOW
195 reference and PDB reference respectively.

196

197

198 **3. Results**

199

200 *3.1 Seawater isotopic composition*

201

202 Measurements of the $\delta^{18}O_w$ values are reported on Fig. 1. This parameter exhibited
203 little seasonal variation with a mean value of -0.1±0.1 ‰. The minimum value was observed
204 in March 2005 (-0.3 ‰), whereas the maximum values occurred in August 2005 and 2006
205 (+0.1 ‰). $\delta^{18}O_w$ values fluctuations are not correlated with temperature ($r = 0.50$; $p < 0.05$),
206 and reflects salinity values ($r = 0.68$; $p < 0.05$) that also remained constant on the breeding
207 site.

208

209 *3.2. Comparison of the shell oxygen isotope ratios with the predicted values at*
210 *isotopic equilibrium*

211

212 Figure 3 reports the time distribution of the $\delta^{18}O_{shell}$ values for four oyster shells. They
213 exhibited a large seasonal range but a small inter-shell variability. Except for the high values
214 in February 2005 (-0.2 to -0.5 ‰), values ranged between +1.5 and +2.2 ‰ in winter and -0.5
215 ‰ and -1.2 ‰ in summer.

216 Determining whether shells precipitate in oxygen isotope equilibrium with seawater
217 requires the estimation of the $\delta^{18}O_{shell}$ value expected at equilibrium into the shell carbonate
218 lattice from the temperature and $\delta^{18}O_w$ values measured in the breeding environment. In the
219 following, we consider isotopic equilibrium in the sense of Kim and O'Neil (1997), which is
220 an apparent equilibrium achieved by most of biogenic carbonates as demonstrated by Daëron
221 et al. (2019). According to temperatures monitored at an subdaily time step (Fig. 2) and $\delta^{18}O_w$

values measured in the oyster area, $\delta^{18}O_c$ values expected at equilibrium (i.e., $\delta^{18}O$ values predicted 1 in Fig. 3) was estimated using the equation of Kim and O'Neil (1997):

$$T = 18030 / (1000 \ln \alpha + 32.17) - 273.15 \quad \text{(equation 1)}$$

$$\text{with } \alpha = (1000 + \delta^{18}O_{shell}) * (1000 + \delta^{18}O_w) \quad \text{(equation 2)}$$

We converted the $\delta^{18}O_{shell}$ expressed in SMOW to PDB value according to the equation of Coplen et al. (1983).

$$\delta^{18}O_c \text{ (SMOW)} = (1.03091) * (\delta^{18}O_{shell} \text{ (PDB)} - 0.25)) + 30.91 \text{ (equation 3)}$$

The $\delta^{18}O_w$ values were monitored in the breeding site by discrete, sub-monthly water sampling, which excludes the interpretation of possible high-resolution fluctuations. But, using Lartaud et al. (2010a) relationship between $\delta^{18}O_w$ values and salinity for various oyster sites from the English Channel and the Atlantic coast of France, including the BDV location, and the subdaily monitoring of salinity in the oyster breeding area, high-resolution $\delta^{18}O_w$ values were calculated as follows:

$$\delta^{18}O_w \text{ (‰)} = 0.22 \text{ S (‰)} - 7.30 \quad \text{(equation 4)}$$

where $\delta^{18}O_w$ is the $\delta^{18}O$ value of seawater in SMOW and S the salinity. This approach was used to obtain a second estimation of $\delta^{18}O$ value expected at equilibrium (i.e., predicted 2 in Fig. 3).

Both models of predicted $\delta^{18}O$ values were in good agreement ($r = 0.99$; $p < 0.05$) (Fig. 3), showing that the use of an estimation of $\delta^{18}O_w$ value through salinity measurements is accurate enough for this type of approach in the environmental settings for which the study was conducted.

We observed on Fig. 3 that during the first six months of the experiment, $\delta^{18}O_{shell}$ values exhibit a significant shift compared to the predicted values at isotopic equilibrium. First, during January and the beginning of February, $\delta^{18}O_{shell}$ values are 0.3 to 1‰ lower than the predicted $\delta^{18}O$. During the second half of February, the isotopic shift increases with shell values more negative by 1.7 to 3 ‰. Then, from March to June, $\delta^{18}O_{shell}$ values remain constant for a given shell, and the shift with the predicted values decreases continuously. Once the organisms reached 1 year old (i.e., during summer 2005), values measured in shells were close to values predicted at isotopic equilibrium.

4. Discussion

4.1. A juvenile isotopic *disequilibrium*

The results observed on Fig. 3 suggest that mineralization occurs out of equilibrium for oxygen isotopes during the younger part of the life of oysters (i.e., < 1 year old). To quantify this disequilibrium compared to theoretical values for calcite and biocalcite, we plotted on Fig. 4 the coefficient of fractionation between water and calcite $\alpha_{c/w}$ as a function of the calculated temperature of mineralization. Two distinct equilibriums were considered: (i) the empirical relationship of Kim and O'Neil (1997) for synthetic calcites, and (ii) that of Watkins et al. (2014) and Daëron et al. (2019) for natural slow growing calcites. These

relationships yield the same dependency on temperature but the Kim and O'Neil (1997) model has a constant offset of -1.5 ‰. The shell portion mineralized during winter and spring 2005 (i.e., during the most juvenile stage of the oysters in the data set), differs greatly from the equilibrium of both the synthetic and slow growing calcites. Various parameters have been proposed to generate isotopic disequilibria in calcites, such as pH of seawater, solution saturation and crystallization rate (Watkins et al., 2014; Devriendt et al., 2017). As these environmental parameters did not differ significantly between winter and spring 2005 (i.e., juvenile oysters) and winter and spring 2006 (i.e., adult oysters), it is unlikely that pH of the seawater or solution saturation could have changed enough to impact the isotopic equilibrium to such a degree. A recent study, which investigated growth patterns of oyster shells from the same spat as the one used in this experiment revealed that during the juvenile part of the shell, growth is characterized by high growth rates (up to 180 µm/day in the hinge area), and severe anomalies in the rhythm of deposition of calcite material (Huyghe et al., 2019). Lower $\delta^{18}O$ values in biogenic material relative to the expected isotopic equilibrium have been suggested to result from kinetic fractionation due to rapid mineralization and the influence of rebalance in the internal fluid pH on the dissolved inorganic carbon species (McConnaughey et al., 1997; Adkins et al., 2003; Dietzel et al., 2009; Uchikawa and Zeebe, 2012). For example, Rollion-Bard et al. (2008) showed that early precipitated calcite is depleted by 3 ‰ compared to secondary calcite in foraminifera tests, due to elevated pH in the calcification fluid. Owen et al. (2002) also showed that for *P. maximus* shells, the $\delta^{18}O_{shell}$ value is more depleted during fast growth rate intervals and these deviations have been interpreted as resulting from kinetic isotope effects. However, in their work, Owen et al. (2002) described a maximum negative shift in the $\delta^{18}O_{shell}$ value of 1 ‰ whereas here the juvenile oyster shells show a maximum negative shift of 3 ‰ (Fig. 3), closer to the isotopic disequilibrium described for corals and foraminifera (Devriendt et al., 2017). Reaching equilibrium between dissolved

carbonate species and water via hydration and hydroxylation reactions requires a minimum residence time in the calcifying fluid estimated at 1h for corals (Rollion-Bard et al., 2003). Staining experiments revealed that calcification occurs in less than 30 min for oysters (Lartaud et al., 2010d). Assuming high growth rates (up to 180 µm / day) in a short period of time during the juvenile stage of oysters (Huyghe et al., 2019), conditions for such strong isotopic disequilibrium exist.

The shift observed between measured and predicted $\delta^{18}O$ values is not constant as the difference between the $\delta^{18}O_{shell}$ values of the three shells and the predicted $\delta^{18}O$ values at equilibrium decreases dramatically until May-June 2005 (~0.5 ‰) (Fig. 3), leading to an $\alpha_{c/w}$ closer to the Kim and O'Neil (1997) equilibrium (Fig.4). This is in agreement with strong but highly variable growth rates during the juvenile stages (Huyghe et al., 2019), leading to periods where conditions to reach equilibria are closer. These results support the model of Coplen et al. (2007) and Daëron et al. (2019) for which only carbonates precipitating at very slow rates can precipitate at isotopic equilibrium.

Contrary to the juvenile phase, the shell portion formed in the adult phase (> 1 year old) appears consistent with the theoretical isotopic equilibrium of Kim and O'Neil (1997), but still differs substantially from the theoretical and measured equilibrium for slow-growing calcites by Watkins et al. (2014) and Daëron et al. (2019), respectively (Fig. 4). This difference implies that the shells calcify too rapidly to achieve DIC-calcite equilibrium. But as the slopes of the equilibrium regression are the same, we conclude that both the equilibrium limit and the kinetic limit of $\alpha_{c/w}$ do not vary significantly with temperature. Although shells do not reach an exact isotopic equilibrium according to Daëron et al. (2019), temperature can be inferred from the Kim and O'Neil (1997) empirical equation.

321 *4.2. Paleoclimatic implications*

322

323 After the first year of life, labeled here as the juvenile phase, our results show that
324 oysters mineralize their shells close to the isotopic equilibrium and thus can accurately reflect
325 the seawater temperatures, assuming an independent estimation of the isotopic composition of
326 seawater. This confirms the use of this type of biogenic material as a promising paleoclimate
327 archive, as revealed by the large bibliography on modern and fossil oysters (Kirby et al.,
328 1998; Surge et al., 2001, 2003; Harding et al., 2010; Lartaud et al., 2010a; Harzhauser et al.,
329 2011; Bougeois et al., 2014; Tynan et al., 2014; Huyghe et al., 2015; Briard et al., 2020).

330 The measured seawater temperatures were plotted versus the difference between
331 $\delta^{18}O_{shell}$ values of oyster shells and the $\delta^{18}O_w$ values estimated through salinity monitoring
332 (equation 4) (Fig. 5). The data for the juvenile phase (February to June 2005) were excluded,
333 as the oysters did not mineralize their shell in isotopic equilibrium during this interval. A
334 negative linear correlation was found between the shell and seawater oxygen isotopes
335 differences ($\delta^{18}O_{shell}$ - $\delta^{18}O_w$) and the seawater temperatures measured by the probes deployed
336 in situ (least mean squares regression, R^2= 0.87, $p < 0.05$, n=60):

337

338 $$T\ (°C) = 15.26(\pm 0.17) - 4.26(\pm 0.22)\ (\delta^{18}O_{shell} - \delta^{18}O_w) \qquad \text{(equation 5)}$$

339

340 With $\delta^{18}O_{shell}$ in PDB and $\delta^{18}O_w$ in SMOW.

341 Different types of equations to link the $\delta^{18}O$ values of calcitic bivalve shells to
342 temperatures exist, with the most currently used are those from Friedman and O'Neil (1977)
343 and Kim and O'Neil, (1997), based on synthetic calcite, and Anderson and Arthur (1983),
344 established from various carbonates including mollusk shells. Figure 6 reports the seawater
345 temperature measured at the BDV over the studied interval compared to the temperatures

346 calculated from the $\delta^{18}O$ values of the four combined shells according to different equations.
347 Kim and O'Neil (1997) (equation 2) and the one issued from this study (equation 5) were
348 used, as well as the equation 6 of Friedman and O'Neil (1977) modified from Tarutani et al.
349 (1969):

350 $$1000 \ln \alpha = (2.78 * 10^6) / T^2 (K) - 2.89 \text{ (equation 6)}$$

351 $$\text{with } \alpha = (\delta^{18}O_{shell\ SMOW} + 1000) / (\delta^{18}O_{w\ SMOW} + 1000) \text{ (equation 7)}$$

352

353 and the equation 8 resulting from Anderson and Arthur (1983):

354

355 $$T (°C) = 16 + 4.14 (\delta^{18}O_c - \delta^{18}O_w) + 0.13 (\delta^{18}O_c - \delta^{18}O_w)^2 \text{ (equation 8)}$$

356

357 Temperatures calculated from the four equations during early phase of the juvenile
358 portion of shells, (i.e., from February to March 2005) is up to ~13 °C warmer than the
359 measured ones. Calculated temperatures differ from the measured temperatures until July
360 2005, due to the isotopic disequilibrium described earlier (Fig. 6). From August 2005, the four
361 equations yield very similar values to measured temperatures, although the Friedman and
362 O'Neil (1977) and Anderson and Arthur (1983) equations exhibit a shift of + 2 °C and +2.5
363 °C in winter 2006 respectively compared to the measured temperatures. This significant
364 positive difference suggests that the Friedman and O'Neil (1977) and Anderson and Arthur
365 (1983) equations are not appropriate enough to reconstruct colder temperatures with oyster
366 shells, at least in temperate climates.

367 These results are of major importance because they show that the choice of T-$\delta^{18}O$
368 values relationship can alter the reconstruction of the seasonal range of seawater temperature
369 from $\delta^{18}O$ analyses. Although the equations of Kim and O'Neil (1997) and the one from this
370 study can deviate slightly from measured values, they generally fit better with the observed

seasonal variations. As the temperatures estimated by these two equations differ on average by only 0.6 °C during winter and 0.9 °C during summer, we suggest using preferentially the equation of Kim and O'Neil (1997) which is already widespread in the literature.

In addition, the reconstructed temperatures based on oxygen isotopes highlitgh that oyster are able to mineralize their shells during winter in seawater temperatures as cold as 5.7 °C. This value is close to the minimum temperature for oyster biomineralization proposed by Ullmann et al. (2010), deduced from stable isotopes analysis, and by Huyghe et al. (2019) from counting growth increment.

5. Conclusions

Oxygen isotope measurements of oyster shells of the species *Magallana gigas* enabled us to identify the parameters controlling the stable isotope composition in their shells. We demonstrate that oysters mineralize their shell at isotopic equilibrium during the adult part of their life (i.e., specimens more than one year old). Oysters shells are thus reliable archives of their living conditions and can be used to accurately reconstruct the seasonal temperature gradient in their environment, even in winter seawater temperatures below 6 °C. The comparison between measured *in situ* temperatures and the temperatures calculated from equations provided by previous studies indicates that the equation of Kim and O'Neil (1997) yields accurate summer and winter temperatures. On the contrary, the equations of Anderson and Arthur (1983) and Friedman and O'Neil (1977) over-estimates winter temperatures by ~ 2 °C, which does not reliably constrain the seasonal range of temperature.

During the juvenile period, (i.e., during the first year of life), an isotopic fractionation was observed for the $\delta^{18}O$ values. This shift is maximum during the younger part of the shell

observed (corresponding to winter here), and is contemporaneous with anomalous high growth peaks. This deviation can be explained by a kinetic isotope effect due to very high growth rates. We thus recommend avoiding the juvenile interval of oyster shells to reconstruct reliable temperatures. Further works are required to investigate if this kind of isotopic disequilibria associated to the juvenile period can be observed in other species than oysters.

Acknowledgments

This work was financially supported by the ANR Amor 'Data Model Reconstruction of the Cenozoic Climate' and the BQR project from Sorbonne Université, 'High frequency to very high frequency recordings of environmental changes to climate by biomineralization.' We thank IFREMER for the use of oyster breeding facilities and for their help with the field work. Special thanks may be due to Brian Mitchell for improving the English of the manuscript.

Contributors

FL, LE, MdR and MRe designed the study. DH, LE, MdR, MRo and FL conducted the field work, and NL and LE carried out the stable isotope analyses. DH and FL wrote the paper. All authors contributed critically to the drafts and gave final approval for publication.

Conflict of interest: The authors declare that they have no conflict of interest.

Ethical approval: All applicable international, national, and/or institutional guidelines for the care and use of animals were followed.

422

References

Adkins, J.F., Boyle, E.A., Curry, W.B., Lutringer, A., 2003. Stable isotopes in deep-sea corals and a new mechanism for "vital effects." Geochim. Cosmochim. Acta 67, 1129–1143.

Anderson, T.F., Arthur, M.A., 1983. Stable isotopes of oxygen and carbon and their application to sedimentologic and paleoenvironmental problems. *In:* ARTHUR, M.A., ANDERSON, T.F., KAPLAN, I.R., VEIZER, J. & LAND, L.S. (eds) Stable Isotopes in Sedimentary Geology. Society of Economic Paleontologists and Mineralogists, Short Course Notes, 10, 1.1-1.151.

Barbin, V., Ramseyer, K., Elfman, M., 2008. Biological record of added manganese in seawater: a new efficient tool to mark in vivo growth lines in the oyster species *Crassostrea gigas*. Int. J. Earth Sci. 97, 193–199.

Bougeois, L., De Rafélis, M., Reichart, G.-J., De Nooijer, L.J., Nicollin, F., Dupont-Nivet, G., 2014. A high resolution study of trace elements and stable isotopes in oyster shells to estimate Central Asian Middle Eocene seasonality. Chem. Geol. 363, 200–212.

Briard, J., Pucéat, E., Vennin, E., Daëron, M., Chavagnac, V., Jaillet, R., Merle, D., de Rafélis, M., 2020. Seawater paleotemperature and paleosalinity evolution in neritic environments of the Mediterranean margin: Insights from isotope analysis of bivalve shells. Palaeogeogr. Palaeoclimatol. Palaeoecol. 543, 109582.

Brigaud, B., Pucéat, E., Pellenard, P., Vincent, B., Joachimski, M.M., 2008. Climatic fluctuations and seasonality during the Late Jurassic (Oxfordian–Early Kimmeridgian) inferred from $\delta^{18}O$ of Paris Basin oyster shells. Earth and Planetary Science Letters, 273(1-2), 58-67.

Coplen, T.B., Kendall, C., Hopple, J., 1983. Comparison of stable isotope reference samples. Nature, 302(5905), 236-238.

Coplen, T.B., 2007. Calibration of the calcite–water oxygen-isotope geothermometer at Devils Hole, Nevada, a natural laboratory. Geochim. Cosmochim. Acta 71, 3948–3957.

448 Daëron, M., Drysdale, R.N., Peral, M., Huyghe, D., Blamart, D., Coplen, T.B., Lartaud, F., Zanchetta,
449 G., 2019. Most Earth-surface calcites precipitate out of isotopic equilibrium. Nat. Commun.
450 10, 429.
451 Devriendt, L.S., Watkins, J.M., McGregor, H.V., 2017. Oxygen isotope fractionation in the $CaCO_3$-
452 DIC-H_2O system. Geochim. Cosmochim. Acta 214, 115–142.
453 Dietzel, M., Tang, J., Leis, A., Köhler, S.J., 2009. Oxygen isotopic fractionation during inorganic
454 calcite precipitation—Effects of temperature, precipitation rate and pH. Chem. Geol. 268,
455 107–115.
456 Epstein, S., Buchsbaum, R., Lowenstam, H., Urey, H.C., 1951. Carbonate-water isotopic temperature
457 scale. Geol. Soc. Am. Bull. 62, 417–426.
458 Epstein, S., Mayeda, T., 1953. Variation of O^{18} content of waters from natural sources. Geochim.
459 Cosmochim. Acta 4, 213–224.
460 Friedman, I., O'Neil, J.R., 1977. Compilation of stable isotope fractionation factors of geochemical
461 interest (Vol. 440). US Government Printing Office.
462 Harding, J.M., Spero, H.J., Mann, R., Herbert, G.S., Sliko, J.L., 2010. Reconstructing early 17^{th}
463 century estuarine drought conditions from Jamestown oysters. Proceedings of the National
464 Academy of Sciences of the United States of America 107, 10549-10554.
465 Harzhauser, M., Piller, W.E., Müllegger, S., Grunert, P., Micheels, A., 2011. Changing seasonality
466 patterns in Central Europe from Miocene Climate Optimum to Miocene Climate Transition
467 deduced from the Crassostrea isotope archive. Glob. Planet. Change 76, 77–84.
468 Hermoso, M., Minoletti, F., Aloisi, G., Bonifacie, M., McClelland, H.L.O., Labourdette, N., Renforth,
469 P., Chaduteau, C., Rickaby, R.E., 2016. An explanation for the ^{18}O excess in
470 Noelaerhabdaceae coccolith calcite. Geochim. Cosmochim. Acta 189, 132–142.
471 Huyghe, D., Merle, D., Lartaud, F., Cheype, E., Emmanuel, L., 2012. Middle Lutetian climate in the
472 Paris Basin: implications for a marine hotspot of paleobiodiversity. Facies 58, 587–604.
473 Huyghe, D., Lartaud, F., Emmanuel, L., Merle, D., Renard, M., 2015. Palaeogene climate evolution in
474 the Paris Basin from oxygen stable isotope ($\delta^{18}O$) compositions of marine molluscs. J. Geol.
475 Soc. 172, 576–587.

476 Huyghe, D., de Rafelis, M., Ropert, M., Mouchi, V., Emmanuel, L., Renard, M., Lartaud, F., 2019.
477 New insights into oyster high-resolution hinge growth patterns. Mar. Biol. 166, 48.
478 https://doi.org/10.1007/s00227-019-3496-2
479 Jones, D.S., Quitmyer, I.R., 1996. Marking time with bivalve shells: oxygen isotopes and season of
480 annual increment formation. Palaios, 340-346.
481 Kim, S.-T., O'Neil, J.R., 1997. Equilibrium and nonequilibrium oxygen isotope effects in synthetic
482 carbonates. Geochim. Cosmochim. Acta 61, 3461–3475.
483 Kirby, M.X., Soniat, T.M., Spero, H.J., 1998. Stable isotope sclerochronology of Pleistocene and
484 Recent oyster shells (*Crassostrea virginica*). Palaios 13, 560–569.
485 Kirby, M.X., 2000. Paleoecological differences between Tertiary and Quaternary *Crassostrea* oysters,
486 as revealed by stable isotope sclerochronology. Palaios, 15(2), 132-141.
487 Kirby, M.X., 2001. Differences in growth rate and environment between Tertiary and Quaternary
488 *Crassostrea* oysters. Paleobiology, 27(1), 84-103.
489 Kobashi, T., Grossman, E.L., Yancey, T.E., Dockery III, D.T., 2001. Reevaluation of conflicting
490 Eocene tropical temperature estimates: Molluskan oxygen isotope evidence for warm low
491 latitudes. Geology 29, 983–986.
492 Langlet, D., Alunno-Bruscia, M., Rafélis, M., Renard, M., Roux, M., Schein, E., Buestel, D., 2006.
493 Experimental and natural cathodoluminescence in the shell of *Crassostrea gigas* from Thau
494 lagoon (France): ecological and environmental implications. Mar. Ecol. Prog. Ser. 317, 143–
495 156.
496 Lartaud, F., Emmanuel, L., De Rafélis, M., Ropert, M., Labourdette, N., Richardson, C.A., Renard,
497 M., 2010a. A latitudinal gradient of seasonal temperature variation recorded in oyster shells
498 from the coastal waters of France and The Netherlands. Facies 56, 13.
499 Lartaud, F., Emmanuel, L., De Rafélis, M., Pouvreau, S., Renard, M., 2010b. Influence of food supply
500 on the $\delta^{13}C$ signature of mollusc shells: implications for palaeoenvironmental reconstitutions.
501 Geo-Mar. Lett. 30, 23–34.
502 Lartaud, F., Chauvaud, L., Richard, J., Toulot, A., Bollinger, C., Testut, L., Paulet, Y.-M., 2010c.
503 Experimental growth pattern calibration of Antarctic scallop shells (*Adamussium colbecki*,

Smith 1902) to provide a biogenic archive of high-resolution records of environmental and climatic changes. J. Exp. Mar. Biol. Ecol. 393, 158–167.

Lartaud, F., de Rafelis, M., Ropert, M., Emmanuel, L., Geairon, P., Renard, M., 2010d. Mn labelling of living oysters: Artificial and natural cathodoluminescence analyses as a tool for age and growth rate determination of *C. gigas* (Thunberg, 1793) shells. Aquaculture 300, 206–217. https://doi.org/10.1016/j.aquaculture.2009.12.018

Latal, C., Piller, W., Harzhauser, M., 2004. Palaeoenvironmental reconstructions by stable isotopes of Middle Miocene gastropods of the Central Paratethys. Palaeogeogr. Palaeoclimatol. Palaeoecol. 211, 157–169. https://doi.org/10.1016/S0031-0182(04)00260-3

Lécuyer, C., Reynard, B., Martineau, F., 2004. Stable isotope fractionation between mollusc shells and marine waters from Martinique Island. Chem. Geol. 213, 293–305.

McConnaughey, T.A., Burdett, J., Whelan, J.F., Paull, C.K., 1997. Carbon isotopes in biological carbonates: Respiration and photosynthesis. Geochim. Cosmochim. Acta 61, 611–622. https://doi.org/10.1016/S0016-7037(96)00361-4

Mette, M.J., Wanamaker, A.D., Jr., Carroll, M.L., Ambrose, W.G., Jr. Retelle, M.J., 2016. Linking large-scale climate variability with Arctica islandica shell growth and geochemistry in northern Norway. Limnology and Oceanography, 61, 748-764.

Mouchi, V., De Rafélis, M., Lartaud, F., Fialin, M., Verrecchia, E., 2013. Chemical labelling of oyster shells used for time-calibrated high-resolution Mg/Ca ratios: a tool for estimation of past seasonal temperature variations. Palaeogeogr. Palaeoclimatol. Palaeoecol. 373, 66-74.

Nedoncelle, K., Lartaud, F., de Rafelis, M., Boulila, S., Le Bris, N., 2013. A new method for high-resolution bivalve growth rate studies in hydrothermal environments. Mar. Biol. 160, 1427–1439. https://doi.org/10.1007/s00227-013-2195-7

Owen, R., Kennedy, H., Richardson, C., 2002. Isotopic partitioning between scallop shell calcite and seawater: effect of shell growth rate. Geochim. Cosmochim. Acta 66, 1727–1737. https://doi.org/10.1016/S0016-7037(01)00882-1

Owen, E.F., Wanamaker, A.D., Feindel, S.C., Schöne, B.R., Rawson, P.D., 2008. Stable carbon and oxygen isotope fractionation in bivalve (*Placopecten magellanicus*) larval aragonite. Geochim. Cosmochim. Acta 72, 4687–4698. https://doi.org/10.1016/j.gca.2008.06.029

Peharda, M., Thébault, J., Markulin, K., Schöne, B.R., Janeković, I., Chauvaud, L., 2019. Contrasting shell growth strategies in two Mediterranean bivalves revealed by oxygen-isotope ratio geochemistry: the case of *Pecten jacobaeus* and *Glycymeris pilosa*. Chemical Geology, 526, 23-35.

Pierre, C., Vangriesheim, A., Laube-Lenfant, E., 1994. Variability of water masses and of organic production-regeneration systems as related to eutrophic, mesotropic and oligotrophic conditions in the northeast Atlantic Ocean. J. Mar. Syst. 5, 159–170. https://doi.org/10.1016/0924-7963(94)90029-9

Purton, L., Brasier, M., 1997. Gastropod carbonate $\delta^{18}O$ and $\delta^{13}C$ values record strong seasonal productivity and stratification shifts during the late Eocene in England. Geology 871–874.

Richardson, C.A., Collis, S.A., Ekaratne, K., Dare, P., Key, D., 1993. The age determination and growth rate of the European flat oyster, *Ostrea edulis*, in British waters determined from acetate peels of umbo growth lines. ICES J. Mar. Sci. 50(4): 493-500

Rollion-Bard, C., Chaussidon, M., France-Lanord, C., 2003. pH control on oxygen isotopic composition of symbiotic corals. Earth Planet. Sci. Lett 215, 265–273.

Rollion-Bard, C., Erez, J., Zilberman, T., 2008. Intra-shell oxygen isotope ratios in the benthic foraminifera genus Amphistegina and the influence of seawater carbonate chemistry and temperature on this ratio. Geochim. Cosmochim. Acta 72, 6006–6014.

Ropert, M., Pien, S., Mary, C., Bouchaud, B., 2007. Rapport REMONOR, Résultats 2006.

Reynolds, D.J., Hall, I.R., Slater, S.M., Scourse, J.D., Halloran, P.R. Sayer, M.D.J., 2017. Reconstructing Past Seasonal to Multicentennial-Scale Variability in the NE Atlantic Ocean Using the Long-Lived Marine Bivalve Mollusk Glycymeris glycymeris. Paleoceanography, 32, 1153-1173.

Salvi, D., Mariottini, P., 2017. Molecular taxonomy in 2D: a novel ITS2 rRNA sequence-structure approach guides the description of the oysters' subfamily Saccostreinae and the genus

558 Magallana (Bivalvia: *Ostreidae*). Zool. J. Linn. Soc. 179, 263–276.
559 https://doi.org/10.1111/zoj.12455
560 Schöne, B.R., Castro, A.D.F., Fiebig, J., Houk, S.D., Oschmann, W., Kröncke, I., 2004. Sea surface
561 water temperatures over the period 1884–1983 reconstructed from oxygen isotope ratios of a
562 bivalve mollusk shell (Arctica islandica, southern North Sea). Palaeogeogr. Palaeoclimatol.
563 Palaeoecol. 212(3-4), 215-232.
564 Schöne, B.R., Fiebig, J., Pfeiffer, M., Gleβ, R., Hickson, J., Johnson, A.L.A., Dreyer, W., Oschmann,
565 W., 2005. Climate records from a bivalved Methuselah (*Arctica islandica*, Mollusca; Iceland).
566 Palaeogeogr. Palaeoclimatol. Palaeoecol. 228, 130–148.
567 Soletchnik, P., Geairon, P., Razet, D., Goulletquer, P., 1996. Physiologie de la maturation et de la
568 ponte chez l'huitre creuse *Crassostrea gigas* (Rapport Ifremer).
569 Spero, H.J., Bijma, J., Lea, D.W., Bemis, B.E., 1997. Effect of seawater carbonate concentration on
570 foraminiferal carbon and oxygen isotopes. Nature 390, 497–500.
571 https://doi.org/10.1038/37333
572 Surge, D., Lohmann, K.C., Dettman, D.L., 2001. Controls on isotopic chemistry of the American
573 oyster, *Crassostrea virginica*: implications for growth patterns. Palaeogeogr. Palaeoclimatol.
574 Palaeoecol. 172, 283–296. https://doi.org/10.1016/S0031-0182(01)00303-0
575 Surge, D.M., Lohmann, K.C., Goodfriend, G.A., 2003. Reconstructing estuarine conditions: oyster
576 shells as recorders of environmental change, Southwest Florida. Estuar. Coast. Shelf Sci.,
577 57(5-6), 737-756.
578 Surge, D., Lohmann, K.C., 2008. Evaluating Mg/Ca ratios as a temperature proxy in the estuarine
579 oyster, *Crassostrea virginica*. J. Geophys. Res. Biogeosci. 113 (G2)
580 Tarutani, T., Clayton, R.N., Mayeda, T.K., 1969. The effect of polymorphism and magnesium
581 substitution on oxygen isotope fractionation between calcium carbonate and water.
582 Geochimica et Cosmochimica Acta, 33(8), 987-996.
583 Tynan, S., Dutton, A., Eggins, S., Opdyke, B., 2014. Oxygen isotope records of the Australian flat
584 oyster (*Ostrea angasi*) as a potential temperature archive. Mar. Geol. 357, 195–209.
585 https://doi.org/10.1016/j.margeo.2014.07.009

586 Tynan, S., Opdyke, B.N., Walczak, M., Eggins, S., Dutton, A., 2017) Assessment of Mg/Ca in
587 *Saccostrea glomerata* (the Sydney rock oyster) shell as a potential temperature record.
588 Palaeogeography, palaeoclimatology, palaeoecology, 484, 79-88.
589 Uchikawa, J., Zeebe, R.E., 2012. The effect of carbonic anhydrase on the kinetics and equilibrium of
590 the oxygen isotope exchange in the CO_2–H_2O system: Implications for $\delta^{18}O$ vital effects in
591 biogenic carbonates. Geochim. Cosmochim. Acta 95, 15–34.
592 https://doi.org/10.1016/j.gca.2012.07.022
593 Ullmann, C.V., Wiechert, U., Korte, C., 2010. Oxygen isotope fluctuations in a modern North Sea
594 oyster (*Crassostrea gigas*) compared with annual variations in seawater temperature:
595 Implications for palaeoclimate studies. Chem. Geol. 277, 160–166.
596 https://doi.org/10.1016/j.chemgeo.2010.07.019
597 Urey, H.C., 1947. The thermodynamic properties of isotopic substances. J. Chem. Soc. Resumed 562–
598 581. https://doi.org/10.1039/JR9470000562
599 Wanamaker, A.D., Jr., Butler, P.G., Scourse, J.D., Heinemeier, J., Eiriksson, J., Knudsen, K.L.
600 Richardson, C.A., 2012. Surface changes in the North Atlantic meridional overturning
601 circulation during the last millennium. Nat Commun, 3, 899.
602 Watkins, J.M., Hunt, J.D., Ryerson, F.J., DePaolo, D.J., 2014. The influence of temperature, pH, and
603 growth rate on the $\delta^{18}O$ composition of inorganically precipitated calcite. Earth Planet. Sci.
604 Lett. 404, 332–343. https://doi.org/10.1016/j.epsl.2014.07.036
605 Wefer, G., Berger, W.H., 1991. Isotope paleontology: growth and composition of extant calcareous
606 species. Mar. Geol., Anoxic Basins and Sapropel Deposition in the Eastern Mediterranean:
607 Past and Present 100, 207–248. https://doi.org/10.1016/0025-3227(91)90234-U
608 Wisshak, M., López Correa, M., Gofas, S., Salas, C., Taviani, M., Jakobsen, J., Freiwald, A., 2009.
609 Shell architecture, element composition, and stable isotope signature of the giant deep-sea
610 oyster *Neopycnodonte zibrowii* sp. n. from the NE Atlantic. Deep Sea Res. Part Oceanogr.
611 Res. Pap. 56, 374–407. https://doi.org/10.1016/j.dsr.2008.10.002
612

613 **Figure caption**

614

615 **Figure 1:** Fluctuation of seawater temperature, salinity (from Huyghe et al., 2019) and $\delta^{18}O$
616 composition of seawater measured above the oyster tables in the Baie des Veys, Normandy,
617 France.

618

619 Figure 2: Illustration of the attribution of an absolute chronological framework to the
620 samplings over the hinge area. A: section of the right part of the hinge area under natural light
621 and illustration of the samplings for stable isotope analyses. The location of the 15 chemical
622 markings are also reported. B: observation of the left section of the hinge under
623 cathodoluminescence allowing for the identification of the Mn^{2+} markings. C:
624 cathodoluminescence profile measured (arbitrary units, AU) along the profile reported in B
625 (white dotted line). High luminescent values correspond to the Mn^{2+} markings. The horizontal
626 axis corresponds to the length measured along the hinge. D: conversion of the length to
627 calendar dates given the dates of the markings and from the counting of the tidal influenced
628 calcitic increments. Horizontal red lines illustrate the fluctuation in the duration of each
629 isotope sample according to the period considered.

630

631 **Figure 3:** Variation through time of the $\delta^{18}O$ of the four shells analyzed. The $\delta^{18}O$ values at
632 isotopic equilibrium predicted from Kim and O'Neil (1997) and calculated from the $\delta^{18}O$ of
633 seawater are shown by the red diamonds ($\delta^{18}O$ predicted 1). The $\delta^{18}O$ values calculated from
634 salinity values are shown by the grey line ($\delta^{18}O$ predicted 2). Note that the vertical (y) axis is
635 inverted.

636

637 **Figure 4**: Correlation between the calculated temperatures from $\delta^{18}O$ of oysters shells using
638 the equation of Kim and O'Neil (1997) and the fractionation coefficient between calcite and
639 water $\alpha_{c/w}$. Comparison is made with the theoretical isotopic equilibrium of Kim and O'Neil
640 (1997) (dotted line) and the equilibrium of slow growing calcites, calculated by Watkins et al.
641 (2014) and Daëron et al. (2019). This comparison highlights that juvenile oyster samples were
642 mineralized out of equilibrium.

643

644 **Figure 5:** Temperature equation proposed according to the oxygen isotopes of oyster shells
645 from for the Baie des Veys. Values before July 2005, when shells mineralized out of isotopic
646 equilibrium during the juvenile period, were excluded from the correlation.

647

648 **Figure 6:** Fluctuation over time of the measured seawater temperatures (from Huyghe et al.,
649 2019) and the temperatures calculated from the $\delta^{18}O$ values of oyster shells using the
650 equations of Friedman and O'Neil (1977), Kim and O'Neil (1997), Anderson and Arthur
651 (1983) and the equation determined from this study.

652

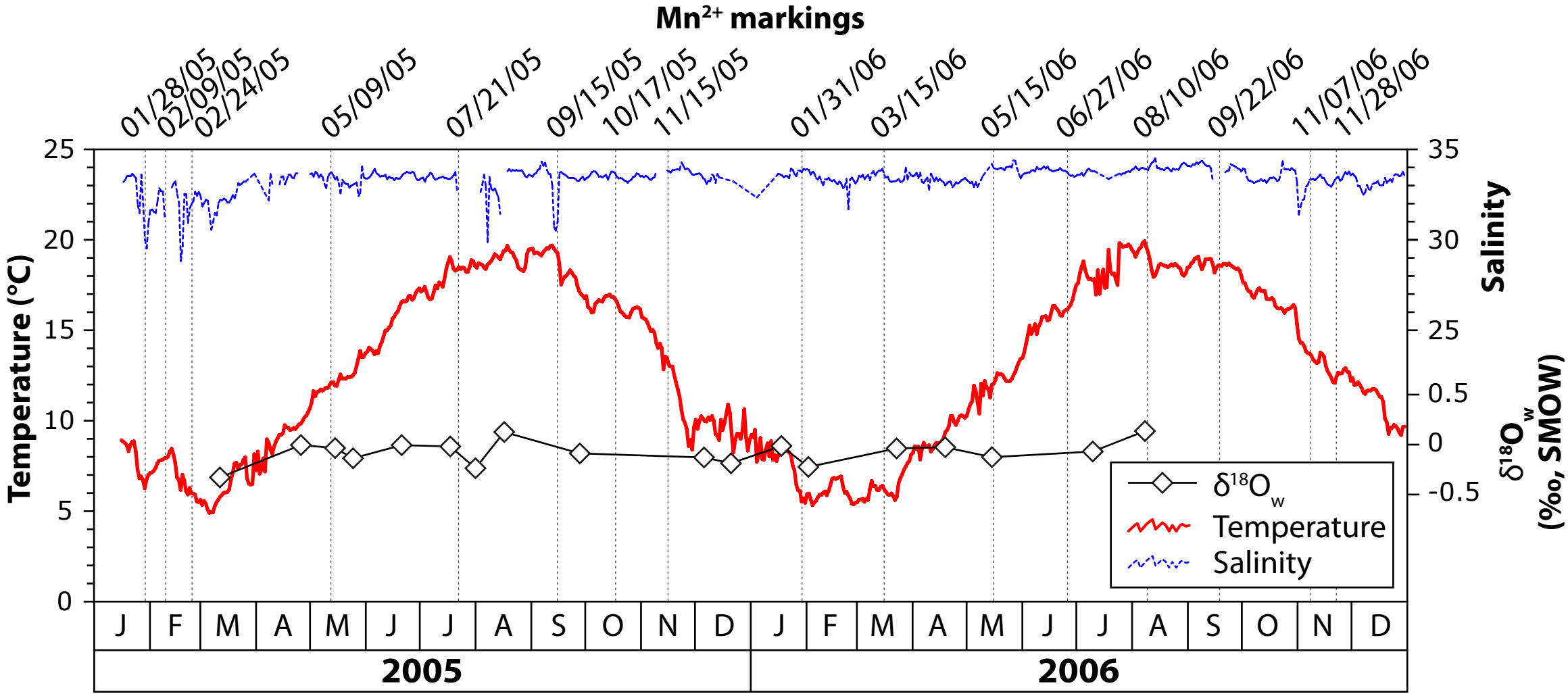
Mn2+ markings
01/28/05
02/09/05
02/24/05
05/09/05
07/21/05
09/15/05
10/17/05
11/15/05
01/31/06
03/15/06
05/15/06
06/27/06
08/10/06
09/22/06
11/07/06
11/28/06
Temperature (°C)
Salinity
δ18Ow (‰, SMOW)
δ18Ow
Temperature
Salinity
J F M A M J J A S O N D J F M A M J J A S O N D
2005
2006

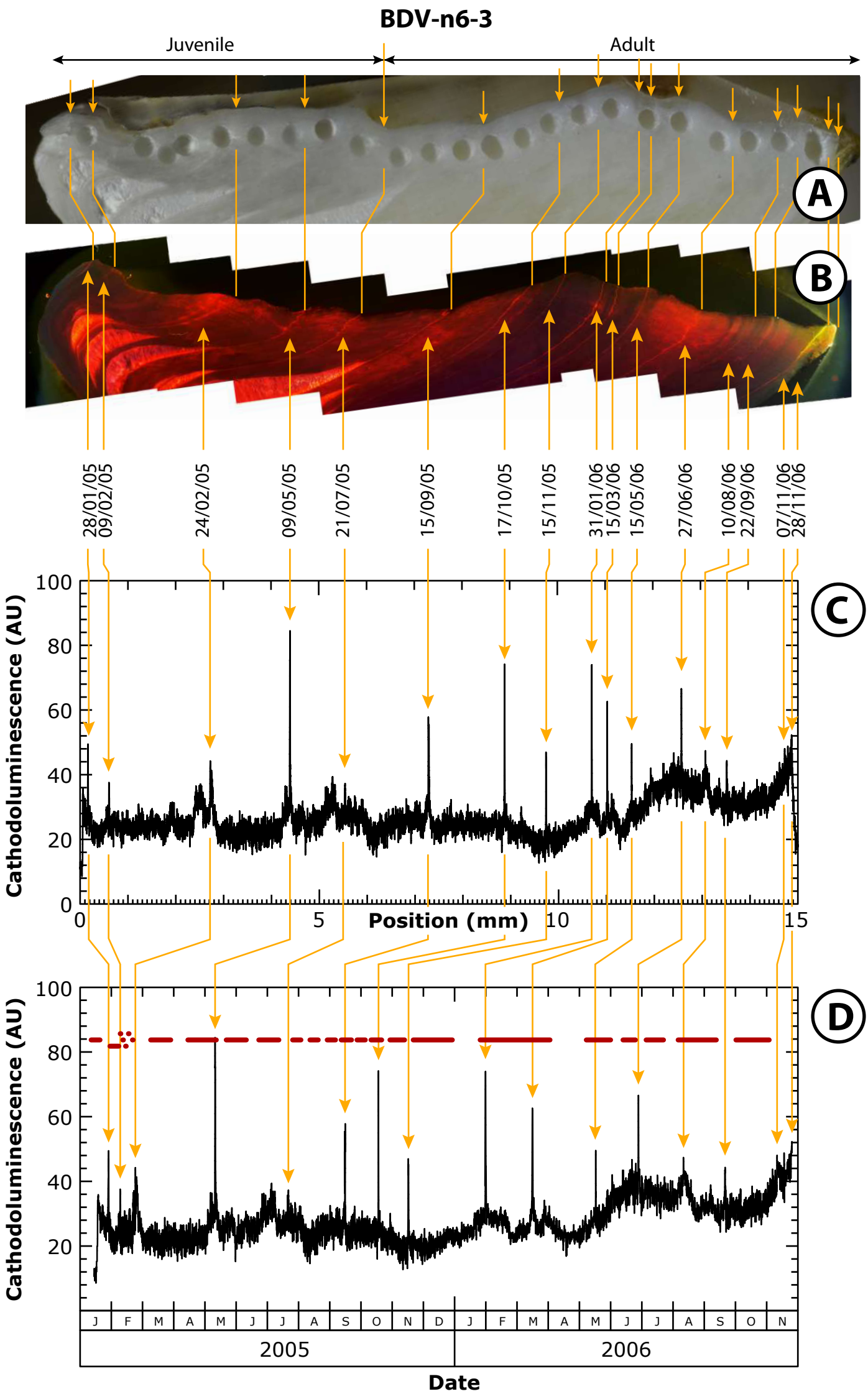
BDV-n6-3
Juvenile
Adult
A
B
28/01/05
09/02/05
24/02/05
09/05/05
21/07/05
15/09/05
17/10/05
15/11/05
31/01/06
15/03/06
15/05/06
27/06/06
10/08/06
22/09/06
07/11/06
28/11/06
C
Cathodoluminescence (AU)
100
80
60
40
20
0
0
5
Position (mm)
10
15
D
Cathodoluminescence (AU)
100
80
60
40
20
J F M A M J J A S O N D J F M A M J J A S O N
2005
2006
Date

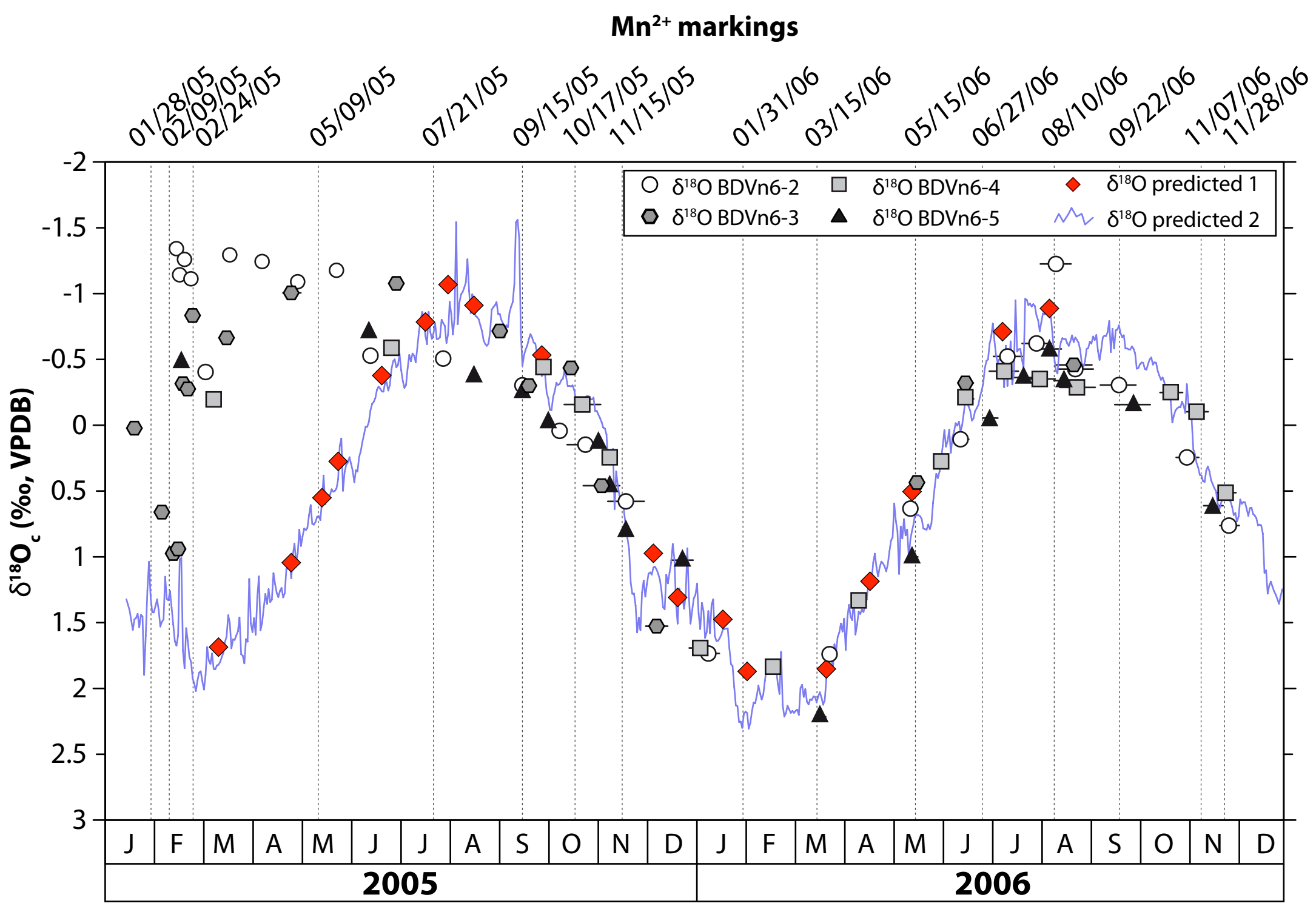
Mn2+ markings
01/28/05
02/09/05
02/24/05
05/09/05
07/21/05
09/15/05
10/17/05
11/15/05
01/31/06
03/15/06
05/15/06
06/27/06
08/10/06
09/22/06
11/07/06
11/28/06
δ18O BDVn6-2
δ18O BDVn6-4
δ18O predicted 1
δ18O BDVn6-3
δ18O BDVn6-5
δ18O predicted 2
δ18Oc (‰, VPDB)
-2
-1.5
-1
-0.5
0
0.5
1
1.5
2
2.5
3
J F M A M J J A S O N D J F M A M J J A S O N D
2005
2006

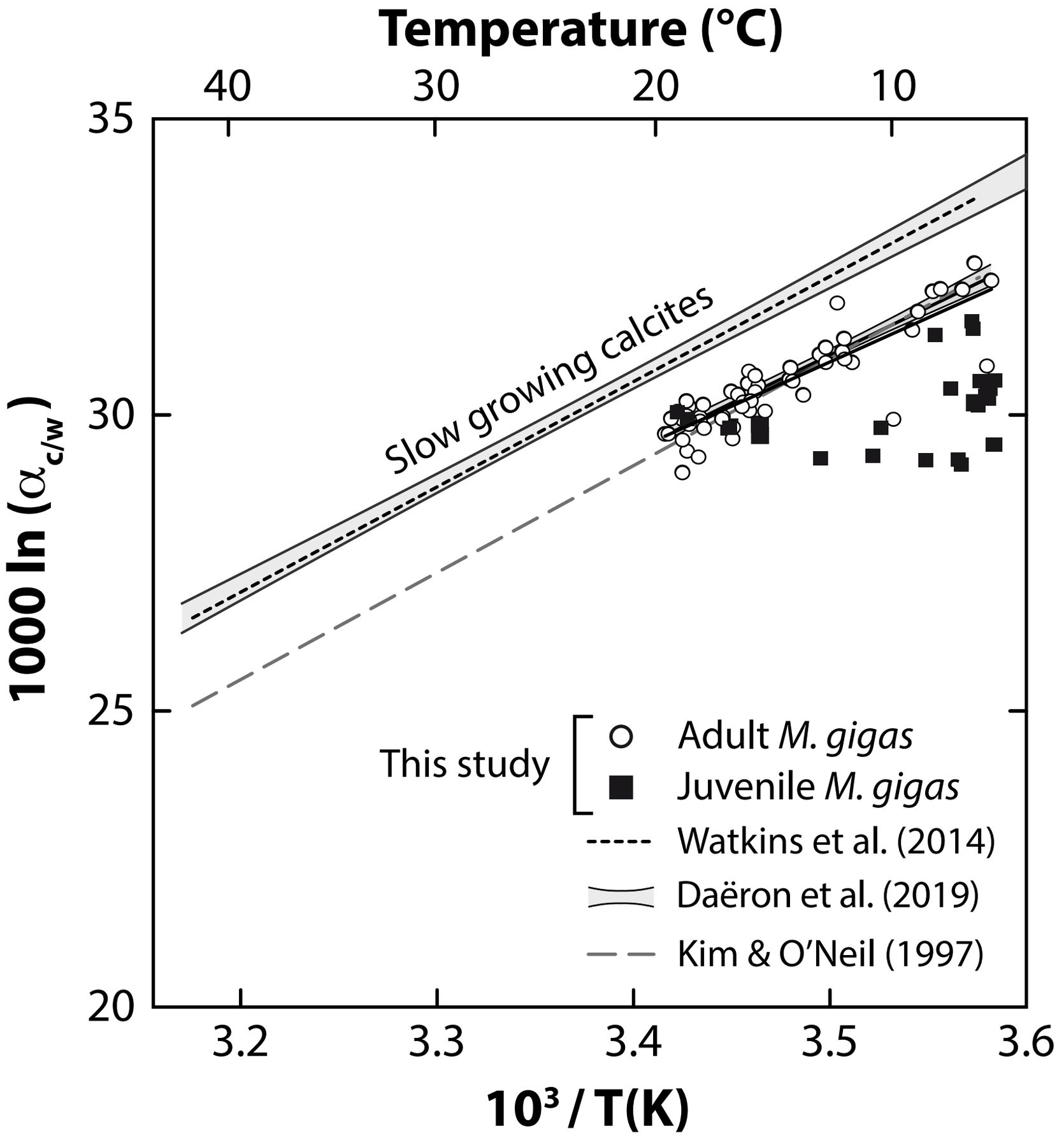
Temperature (°C)
40
30
20
10
35
30
25
20
1000 ln ($\alpha_{c/w}$)
Slow growing calcites
This study
Adult *M. gigas*
Juvenile *M. gigas*
Watkins et al. (2014)
Daëron et al. (2019)
Kim & O'Neil (1997)
3.2
3.3
3.4
3.5
3.6
10^3 / T(K)

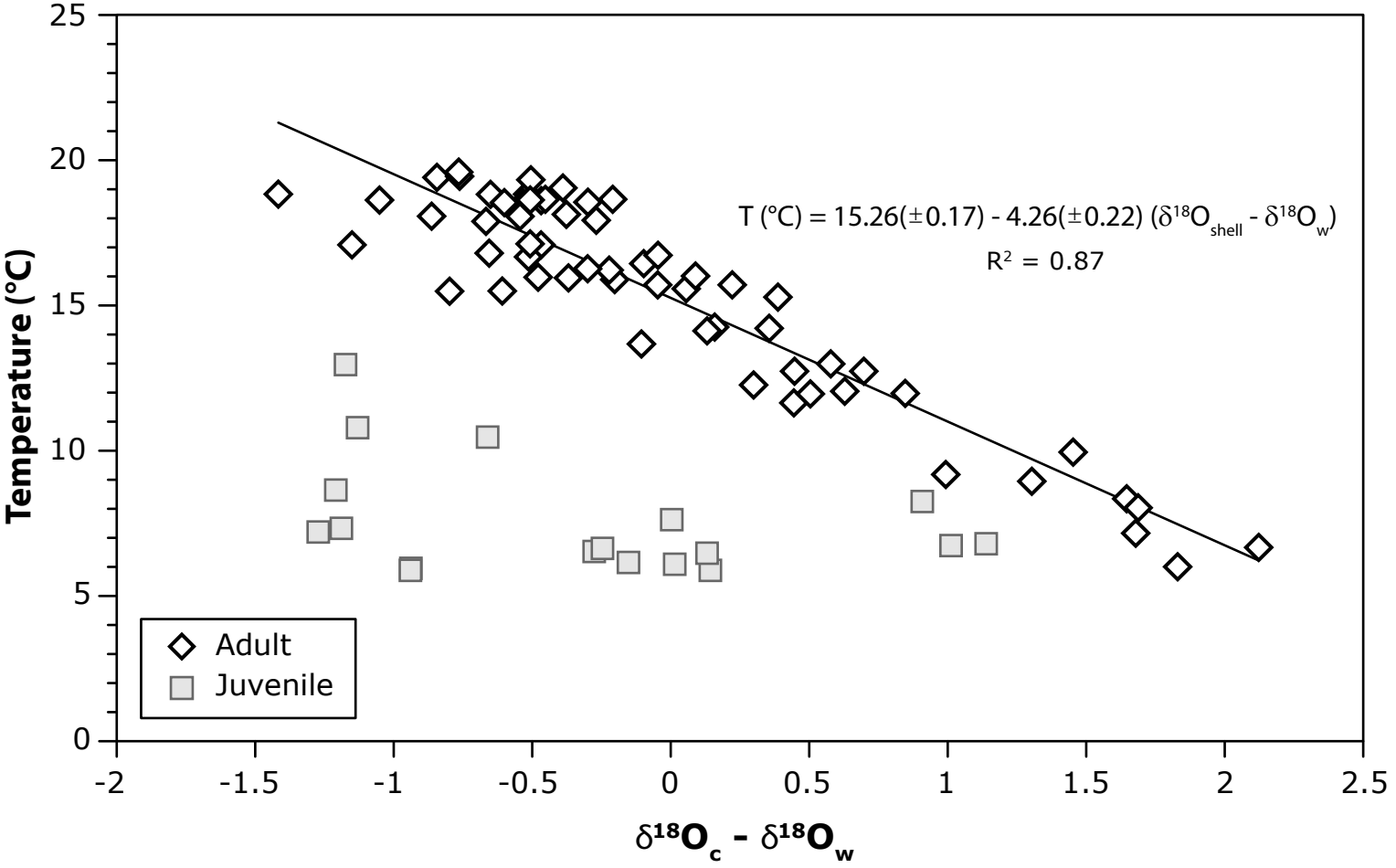
Temperature (°C)
25
20
15
10
5
0
-2
-1.5
-1
-0.5
0
0.5
1
1.5
2
2.5
δ18Oc - δ18Ow
T (°C) = 15.26(±0.17) - 4.26(±0.22) (δ18Oshell - δ18Ow)
R2 = 0.87
Adult
Juvenile

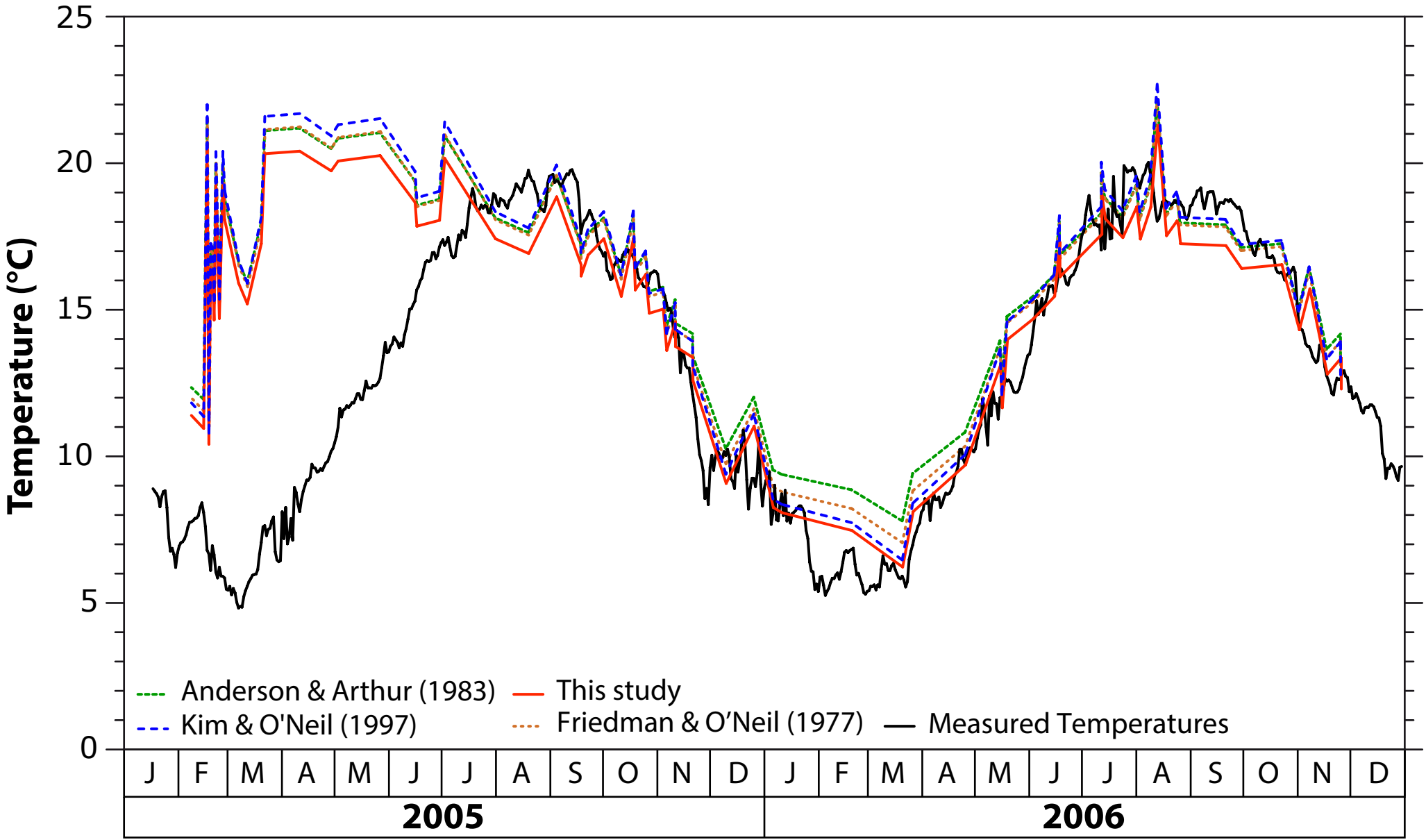
Temperature (°C)
25
20
15
10
5
0
Anderson & Arthur (1983)
Kim & O'Neil (1997)
This study
Friedman & O'Neil (1977)
Measured Temperatures
J F M A M J J A S O N D J F M A M J J A S O N D
2005
2006